European Journal of Pharmaceutics and Biopharmaceutics 103 (2016) 43–50

Contents lists available at ScienceDirect

European Journal of Pharmaceutics and Biopharmaceutics

journal homepage: www.elsevier.com/locate/ejpb

Microneedle-mediated delivery of donepezil: Potential for improved treatment options in Alzheimer's disease

Mary-Carmel Kearney, Ester Caffarel-Salvador, Steven J. Fallows, Helen O. McCarthy, Ryan F. Donnelly *

School of Pharmacy, Queen's University Belfast, 97 Lisburn Road, Belfast BT9 7BL, UK

ARTICLE INFO

Article history:
Received 6 January 2016
Revised 3 March 2016
Accepted in revised form 23 March 2016
Available online 24 March 2016

Keywords:
Microneedles
Transdermal drug delivery
Donepezil hydrochloride
Films
Patch

ABSTRACT

Transdermal drug delivery is an attractive route of drug administration; however, there are relatively few marketed transdermal products. To increase delivery across the skin, strategies to enhance skin permeability are widely investigated, with microneedles demonstrating particular promise. Hydrogel-forming microneedles are inserted into the skin, and following dissolution of a drug loaded reservoir and movement of the drug through the created channels, the microneedle array is removed intact, and can then be readily and safely discarded. This study presents the formulation and evaluation of an integrated microneedle patch containing the Alzheimer's drug, donepezil hydrochloride. The integrated patch consisted of hydrogel-forming microneedles in combination with a donepezil hydrochloride containing film. Formulation and characterisation of plasticised films, prepared from poly(vinylpyrrolidone) or poly (methyl vinyl ether co-maleic anhydride/acid) (Gantrez®) polymers, is presented. Furthermore, *in vitro* permeation of donepezil hydrochloride across neonatal porcine skin from the patches was investigated, with 854.71 μg ± 122.71 μg donepezil hydrochloride delivered after 24 h, using the optimum patch formulation. Following administration of the patch to an animal model, plasma concentrations of 51.8 ± 17.6 ng/mL were obtained, demonstrating the success of this delivery platform for donepezil hydrochloride.

1. Introduction

Microneedles (MNs)[1] are minimally invasive devices capable of penetrating the skin's *stratum corneum*, overcoming its barrier properties. This increases the potential for transdermal delivery of a greater number of drugs, as the prerequisite for substances to have specific physicochemical properties for passive transdermal delivery is negated [1]. Transdermal drug delivery has numerous well documented benefits, including avoidance of first-pass hepatic metabolism, the offer of controlled drug delivery, and reduction in gastrointestinal side-effects and is particularly useful for patients with dysphagia [2]. Since description of the first studies exploring the delivery capabilities of MNs, interest in the field has grown exponentially [3–5]. It has been acknowledged, that of the various strategies to enhance transdermal drug delivery, MN technology is progressing with the greatest promise, with human studies already conducted for the delivery of vaccines *via* this mechanism [6].

The various MN types have been extensively discussed, with the benefits and limitations of each type identified [7,8]. Hydrogel-forming MNs have several unique characteristics which make them suitable for a broad range of drug delivery applications. They are hard in the dry state, enabling successful insertion into the skin. Once *in situ*, they imbibe interstitial fluid and swell. This creates a porous network through which drug contained within a reservoir can diffuse from, and move into the dermal microcirculation (Fig. 1) [9]. Modification of MN swelling confers the ability to control rate of drug release. The drug reservoir is formulated independently of the MNs allowing further manipulation of the drug delivery system and, as a result, drug loading is not restricted to what can be contained within the needles themselves; a distinct advantage in comparison with dissolving and coated MNs. Aside from MN studies involving the delivery of a vaccine, the majority of drugs used have been for exemplar purposes. As the field continues to progress, the question as to what other applications MNs may have, has been asked [10].

The benefit of transdermal products in Alzheimer's disease has been recognised with a rivastigmine patch currently on the market. This product had an excess of US $400 million in sales in 2014, highlighting the commercial success of transdermal products for patients suffering from this condition [11]. Anti-Alzheimer's drugs

* Corresponding author at: School of Pharmacy, Queen's University Belfast, Medical Biology Centre, 97 Lisburn Road, Belfast BT9 7BL, UK.
E-mail address: r.donnelly@qub.ac.uk (R.F. Donnelly).

[1] MNs = Microneedles.

http://dx.doi.org/10.1016/j.ejpb.2016.03.026
0939-6411/

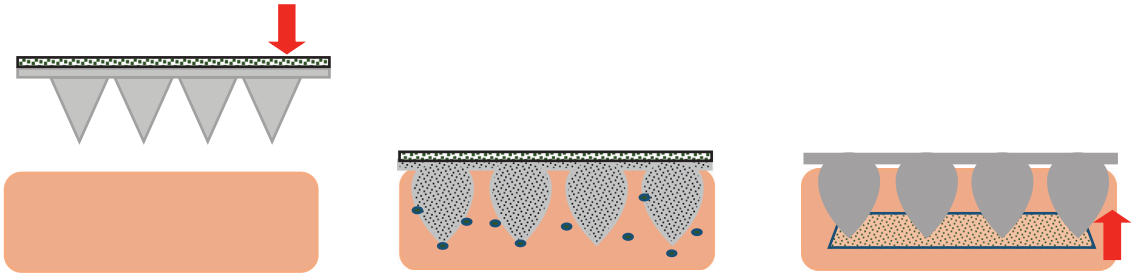

Fig. 1. Schematic representation of the mechanism of action of hydrogel-forming MNs in combination with a drug loaded reservoir.

are therefore a logical therapeutic choice when considering a clinically useful MN product. Donepezil (Fig. 2) (2-[(1-benzylpiperidin-4-yl)methyl]-5,6-dimethoxy-2,3-dihydro-1H-inden-1-one) is an acetylcholinesterase inhibitor used in the treatment of mild to moderate dementia in Alzheimer's disease. Alzheimer's disease is the most prevalent form of dementia, which affects 835,000 people in the UK. With an ageing population and improved diagnoses, the number of people suffering from this condition, in the UK, is predicted to increase to over 2 million by 2051 [12]. Alzheimer's disease is associated with a reduction in certain cerebral neurotransmitters, including acetylcholine. The aim of donepezil treatment is to inhibit the hydrolysis of acetylcholine, thereby increasing its concentration in the synaptic cleft, and consequently, improving neurotransmission. It has been hypothesised that donepezil formulated as a transdermal patch, similar to rivastigmine, could provide significant patient benefit. A particular advantage of avoiding the gastrointestinal (GI) tract, by using a patch formulation, is a reduction in GI related side effects. Further to this, dysphagia is a common symptom of Alzheimer's disease, frequently hindering treatment with oral preparations [11]. Poor compliance to medication regimens amongst patients suffering from Alzheimer's disease is commonly reported, with one study finding that, following six months of oral donepezil treatment, only 52% of patients were fully adherent [12]. It has been shown that compliance in the elderly population is greater with transdermal patches in comparison with the oral form [13,14].

The base form of donepezil has a Log *P* of 3.08–4.11 and does not passively traverse the skin at clinically relevant levels [15,16]. To enhance transdermal delivery, various methods have been employed, mainly penetration enhancers [16,17] and iontophoresis [18]. These methods have investigated the delivery of both the free base form of the drug and the hydrochloride (HCl) salt. As it has been demonstrated that MNs can significantly increase the transdermal delivery of small, water soluble drug substances, we hypothesise that MNs could be used to facilitate the transdermal delivery of donepezil HCl (molecular weight: 433.97 g/mol). Our previous work has largely focused on the delivery of compounds with representative physicochemical properties using this novel MN system [9]. In contrast this study examines the modification and development, of this delivery system for a therapeutically relevant compound. The aim of the current study was to develop a novel 'integrated' MN patch consisting of a donepezil HCl loaded film and hydrogel-forming MNs for enhanced *in vitro* and *in vivo* transdermal delivery of this Alzheimer's drug.

2. Materials and methods

2.1. Materials

Gantrez® AN-139 and S-97, copolymers of methyl vinyl ether and maleic anhydride and methyl vinyl ether and maleic acid, respectively (PMVE/MAH and PMVE/MA, with molecular masses

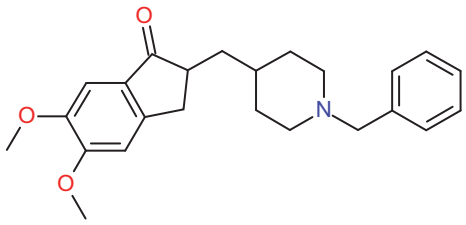

Fig. 2. Molecular structure of donepezil.

of 1,080,000 and 1,500,000 respectively) were gifts from Ashland, Kidderminster, UK. Poly(ethylene glycol) (PEG MW 10,000 Da), poly(vinylpyrrolidone) (PVP, MW 58,000 g/mol), glycerol, tripropylene glycol methyl ether (TPME), triethylamine and HPLC grade methanol and acetonitrile were purchased from Sigma Aldrich, Dorset, UK. Donepezil HCl was purchased from TCI UK Ltd., Zwijndrecht, Belgium. All other chemicals used were of analytical reagent grade.

2.2. Fabrication of hydrogel-forming MNs

MN arrays were fabricated from aqueous blends containing 15% w/w Gantrez® S-97, 7.5% w/w PEG, 10,000 and 3% w/w Na_2CO_3 as previously described [19]. Approximately 500 mg of blend was poured into 11 × 11 MN moulds and these were centrifuged at 2205 g for 15 min and dried at room temperature for 48 h. Crosslinking was induced *via* an esterification reaction, by heating the MNs at 80°C for 24 h [20]. Following this 24 h heating process, moulds were allowed to cool and the arrays extracted, with sidewalls formed by the moulding process removed using a heated blade. The final arrays produced contained 121 needles perpendicular to the base and of conical shape (600 μm in height, with base width of 300 μm and 150 μm interspacing on a 0.49 cm^2 patch).

2.3. Pharmaceutical analysis of donepezil hydrochloride

To analyse donepezil HCl delivered *in vitro*, a reverse phase high performance liquid chromatography (RP-HPLC) method was developed. An Agilent 1200 series system (Agilent Technologies UK Ltd., Stockport, UK) was used for analysis. The column used was a Phenomenex Luna® C18 (ODS1) column (150 mm × 4.6 mm internal diameter, 5 μm packing, Phenomenex, Cheshire, UK) with UV detection at 272 nm (run time per sample = 6 min). The mobile phase consisted of 65:34.5:0.5 acetonitrile:0.025 M potassium dihydrogen phosphate buffer (pH 3.0):triethylamine, at a flow rate of 1 mL/min. Column temperature was maintained at 25°C and injection volume was 20 μL. Agilent ChemStation® Software B.02.01 was used for chromatogram analysis. Correlation analysis along with least squares linear regression analysis was performed on the calibration curves generated, enabling determination of the equations of the line and their coefficients of determination. Limits

of detection (LoD) and limits of quantification (LoQ) were determined using a method based on the standard deviation of the response and the slope of the representative calibration curve, as described in the guidelines from ICH [21]. The LoD of each method was determined as follows, using Eq. (1):

$$\mathrm{LoD} = \frac{3.3\sigma}{S} \quad (1)$$

where σ is the standard deviation of the response data used to construct the regression line and S is the slope of that line. Similarly, the LoQ was determined using Eq. (2):

$$\mathrm{LoQ} = \frac{10\sigma}{S} \quad (2)$$

For analysis of donepezil HCl in plasma samples, the above RP-HPLC method was optimised to facilitate donepezil HCl detection at lower concentrations. A Waters™ XSelect CSH C18 column (75 mm × 3 mm internal diameter, 2.5 μm packing) was used for the separation with fluorescence detection at λ excitation 318 nm and λ emission 390 (run time = 5 min). The mobile phase consisted of 30:70 acetonitrile:0.025 M potassium dihydrogen phosphate buffer (pH 3.0) at a flow rate of 0.7 mL/min. The injection volume was 10 μL. Agilent ChemStation® Software B.02.01 was used for chromatogram analysis.

2.4. Preparation of donepezil HCl loaded films

Donepezil HCl containing films were prepared by using a casting method, from aqueous blends of PMVE/MAH, PMVE/MA or PVP polymers and a plasticiser, as detailed in Table 1. Required amounts of donepezil HCl were added directly into the aqueous blends. An aliquot of drug loaded aqueous blend was cast in either a silicone mould (5 cm × 5 cm) or a mould consisting of a stainless steel frame secured on a Perspex® base (5 cm × 2 cm). The mould was placed on a levelled surface, allowing even spreading of the formulation. The cast blend was then dried at room temperature for 48 h.

2.5. Physical characterisation of donepezil HCl containing films

Film thickness was measured using a digital micrometer (Hilka, ProCraft, Surrey, UK) and a TA-XT2 Texture Analyser (Stable Microsystems, Haslemere, UK) was used for determination of tensile strength, percentage elongation and calculation of Young's Modulus. Film strips (50 mm × 5 mm) were secured between two grips set at 20 mm spacing and a cross-head speed of 0.5 mm/s was used.

2.6. Donepezil HCl film recovery

Segments (1 cm^2) of donepezil HCl-containing films were dissolved in 100 mL of PBS stirred at 400 rpm at 37°C. Following dissolution, samples were diluted appropriately and filtered using 0.22 μm Millex®-GS syringe filter (Merck Millipore Ltd., Carrigtwohill, Ireland) and analysed using the RP-HPLC with UV detection method, as outlined above.

2.7. Donepezil-containing films dissolution study

Films measuring 1 cm^2 were weighed, immersed in 30 mL PBS (pH 7.4) and removed at pre-defined time-intervals. Upon removal, excess PBS was removed by blotting with filter paper and samples reweighed until the point of complete film dissolution.

Table 1
Formulations for donepezil containing films.

Formulation	% w/w Gantrez AN 139	% w/w Gantrez S97	% w/w PVP K29/32	% w/w TPM	% w/w PEG 400	% w/w Glycerol
F1	15	–	–	7.5	–	–
F2	–	–	15	–	5	–
F3	–	–	15	–	–	5
F4	–	10	–	5	–	–
F5	–	15	–	7.5	–	–
F6	10	–	–	5	–	–

2.8. In vitro donepezil drug delivery studies

Modified Franz cell chamber system was used to assess the permeation of donepezil HCl from films in combination with hydrogel-forming MNs, across dermatomed, neonatal porcine skin (Fig. 3). Skin samples were obtained from stillborn piglets and immediately (<24 h after birth) excised, trimmed to a desired thickness (approximately 350 μm) using an electric dermatome (Integra Life Sciences™, Padgett Instruments, NJ, USA) and frozen at −20°C until use. MN arrays (11 × 11 needle density, 600 μm height, 300 μm width at base and 150 μm interspacing) were inserted using manual pressure with 20 μL PBS placed on the array to promote adhesion of the films containing approximately 2 mg donepezil HCl to the MN baseplate. A cylindrical 5.0 g stainless steel weight was placed on top of the MN array to prevent MN expulsion, and the donor compartment of the apparatus was clamped onto the receiver compartment. The donor compartment and sampling arm were sealed using Parafilm M®. The receiver compartment contained PBS (pH 7.4) degassed prior to use and thermostated to 37 ± 1°C. Syringes (1.0 mL) with 8.0 cm needles were used to remove 200 μL of the Franz cell contents at pre-determined time intervals and 200 μL of pre-warmed PBS was subsequently added to replace this. Control Franz cells were assembled in the same manner, but without the application of MN arrays. Instead, the drug loaded films were applied directly to the skin.

2.9. In vivo drug delivery studies

Male Sprague–Dawley rats weighing 260.8 ± 13 g, were allowed to acclimatise for 7 days prior to experimentation. To minimise interference of rat hair with MN application, it was removed from the back region 24 h prior to the experiment. Firstly, an animal hair clipper was used to remove the bulk of hair with depilatory cream (Boots Expert® The Boots Company PLC, Nottingham, UK) then applied to remove any residual hair. Following this, there was a 24 h recovery period to ensure complete restoration of skin barrier function [9,22]. To facilitate MN application, rats were anesthetised using gas anaesthesia (2–4% isoflurane in oxygen). Rat skin was pinched and four MN arrays, mounted on an adhesive foam border (TG Eakin Ltd., Comber, Co Down, UK), were inserted into the backs of each rat using firm finger pressure. Donepezil HCl-loaded films (F1) with a drug loading of either 5 mg/kg or 2.5 mg/kg were applied to the back of the arrays covering the area exposed to the MNs. To secure the integrated patch in place, an occlusive transdermal backing consisting of Duro-tak® adhesive grade 387-2054 and Scotchpak™ film (3 M UK Plc, Bracknell, Berkshire, UK) was applied on top of the arrays and this was further wrapped in place using Micropore® tape (3M UK Plc, Bracknell, Berkshire, UK). Blood samples were taken *via* tail vein bleeds at pre-defined time intervals: 1, 2, 4, 6 and 24 h with a maximum of 200 μL collected at each sampling point. These samples were processed as

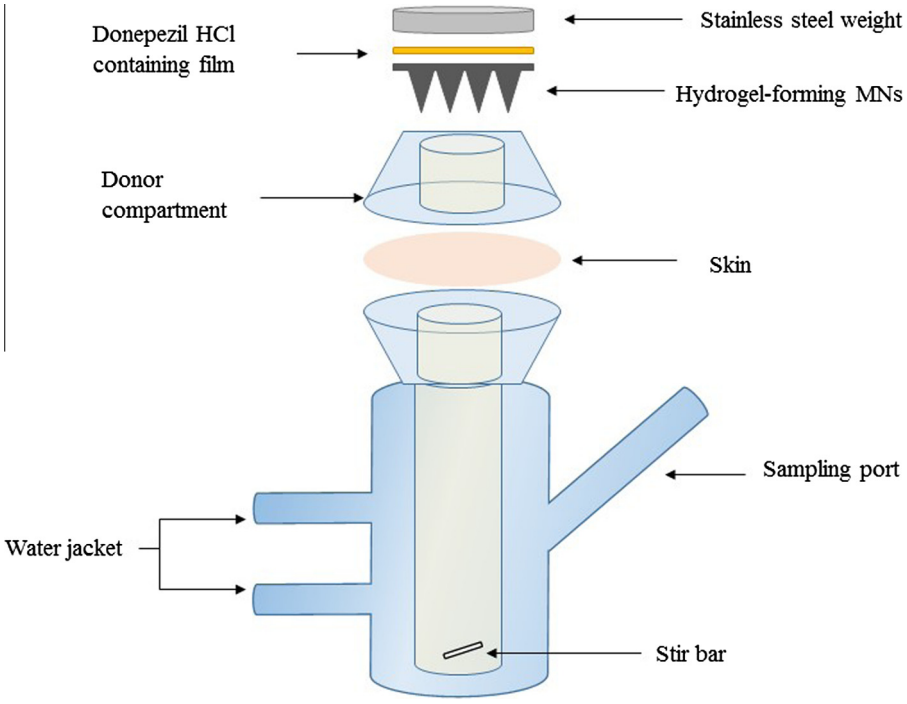

Fig. 3. Schematic representation of modified Franz cell chamber system for *in vitro* testing of donepezil HCl permeation across neonatal porcine skin using hydrogel-forming MNs.

detailed below prior to RP-HPLC analysis. Approval for animal experiments was obtained from the Committee of the Biological Research Unit, Queen's University Belfast. The work was carried out under the Project Licence PPL 2678 and the Personal Licence PIL 1465. All *in vivo* experiments were conducted according to the policy of the federation of European Laboratory Animal Science Associations and the European Convention for the protection of vertebrate animals used for experimental and other scientific purposes, with implementation of the principles of the 3R's.

2.10. Extraction of plasma and drug

Healthy male Sprague–Dawley rats were culled and blood was collected into heparinised tubes following cardiac puncture. This control blood was used for assay method development. To separate plasma from the blood, the tubes were centrifuged at 3000 relative centrifugal force (RCF) for 10 min at 4°C. 180 μL of plasma was subsequently aliquoted into 1.5 mL Eppendorf® tubes and stored at −80°C until used. Aliquots (20 μL) of donepezil HCl working standard solutions were added to 180 μL blank plasma and vortexed for 10 s. Acetonitrile (500 μL) was then added to the plasma/standard mixture and vortex-mixed for 10 min. This was followed by centrifugation at 14,000 RCF for 10 min at 4°C. The supernatant was removed from the Eppendorf® tube and transferred to a disposable glass culture tube. The acetonitrile extraction procedure was repeated to ensure optimum extraction of donepezil HCl with the supernatant again transferred to the culture tube. The sample extract was then dried under a stream of nitrogen at 35°C for 50 min using a Zymark TurboVap® LV Evaporator Workstation (McKinley Scientific, Sparta, NJ, USA). The residue was then reconstituted in 200 μL PBS (pH 7.4) and collected into an Eppendorf®. This was vortex-mixed for 30 s and centrifuged at 14,000 RCF for 10 min at room temperature. The supernatant was transferred into an Agilent® HPLC vial and 10 μL was injected onto the HPLC column.

2.11. Statistical analysis

A One-way ANOVA test was used to compare the various film formulations in terms of strength, elongation and donepezil HCl recovery. Where appropriate, an unpaired *t*-test or Mann–Whitney U test was used to statistically compare the results of *in vitro* data and *in vivo* data. In all cases, $p < 0.05$ denoted significance. Statistical analysis was carried out using GraphPad Prism® version 5.0 (GraphPad Software Inc., San Diego, California).

3. Results

3.1. Pharmaceutical analysis of donepezil hydrochloride

HPLC methods for the quantification of donepezil HCl, in either PBS or plasma, were developed and validated according to ICH guidelines. Limits of quantification and detection are presented in Table 2 (i) and (ii) respectively. Typical HPLC traces for each method are displayed in Fig. 4a and b.

3.2. Physical characterisation of donepezil HCl containing films

Donepezil HCl containing films were characterised in terms of dimension uniformity, tensile strength, percentage elongation and Young's modulus. Details of the film formulations are documented in Table 1. All films were of similar thickness with an average thickness of 0.41 mm ± 0.05 mm. No significant difference was found between any of the formulations apart from F6, which displayed higher tensile strength ($p < 0.05$) (Fig. 5a) and much less elasticity ($p < 0.05$), as determined by % elongation, (Fig. 5b) in comparison with the other formulations.

3.3. Donepezil HCl film recovery

Films containing a known mass of donepezil HCl were dissolved in PBS and the concentration of the drug contained within was

Table 2
Calibration curve properties for donepezil HCl quantification in (i) PBS (pH 7.4) and (ii) rat plasma and limits of detection and quantification for donepezil HCl.

Slope	y-Intercept	r^2	LoD (μg/mL)	LoQ (μg/mL)
9.3854	0.7042	0.9999	0.11	0.52
329	0.0426	0.9959	0.01	0.03

determined. Recovery of donepezil HCl from F6 was not assessed as mechanical properties of this formulation were deemed not suitable for this application. Recovery from all investigated films was over 90% with an average recovery of 96.96% ± 6.56% (Fig. 5c). This suggests that there were no meaningful compatibility issues between the drug and film components.

3.4. Donepezil-containing films dissolution study

Films were dissolved in PBS to determine an estimated dissolution rate. Films based on PMVE/MAH and PMVE/MA were found to initially swell with subsequent dissolution. Contrastingly, films composed of PVP dissolved rapidly, with complete dissolution having occurred within 15 min, almost 4-times faster than PVME/MA and PVME/MAH films. Complete film dissolution for all formulations occurred within 40 min of immersion into PBS (Fig. 5d).

3.5. In vitro donepezil drug delivery studies

Permeation of donepezil HCl across neonatal porcine skin was significantly enhanced by using MN arrays in comparison with the control set-up ($p < 0.05$). The composition of the donepezil HCl film reservoir impacts on the total permeation. Following application of the combined MN and film formed from F1 for 24 h, 854.71 μg ± 122.71 μg donepezil HCl was delivered, in comparison with 266.81 μg ± 172.68 μg delivered from the patch containing a PVP based film (F3). Permeation from films prepared from four of the six test formulations was investigated; however data presented include permeation from F1 and F3. These are presented as these represent the maximum delivery of donepezil HCl from a Gantrez® based film and a PVP based film. Permeation from the other films was lower and these formulations were therefore not considered for the *in vivo* study. F4 was not investigated at this stage as donepezil HCl recovery was 90.2% ± 4.2%. As stated previously, F6 was not tested after considering the results of its physical properties. F1 The permeation rate of donepezil HCl was calculated using Eq. (3) from the slopes of the linear portions of the permeation profiles.

$$\text{Permeation rate} = \frac{dM}{S \times dt} \tag{3}$$

where M is the mass of donepezil HCl permeated through the MNs, of unit cross-sectional area (S) in unit time (t). For the Gantrez® based integrated patch, the permeation rate was 172.2 μg/h/cm^2 ± 34.9 μg/h/cm^2 between 2 and 6 h and 269.9 μg/h/cm^2 ± 105.4 μg/h/cm^2 between 1 and 4 h for the PVP based integrated patch. Although the permeation rate is higher for the PVP based patch over the linear period, following this the permeation of donepezil HCl rapidly plateaus (after 4 h), with significantly less permeated from this system by 24 h ($p < 0.05$). It is noticeable that the error associated with the permeation rate of the PVP based film is considerably large and error is often reported with the use of biological membranes such as porcine skin [23]. Further to this, it is acknowledged that the permeation rates calculated are an approximation, as, with hydrogel MNs the area of the array increases as the system swells; this too may potentially contribute to error. In terms of percentage delivery, after 24 h 34.63% ± 3.70% of donepezil HCl contained within the Gantrez® based patches was delivered in comparison with 13.11% ± 4.83% from PVP based films. When compared to the control setup, both MN patches demonstrated enhanced delivery ($p < 0.05$) (Fig. 6).

3.6. In vivo drug delivery and quantification

Each rat had a total of four integrated MN patches applied to their back with three rats administered 2.5 mg/kg donepezil HCl, and three administered 5 mg/kg donepezil HCl. As can be seen from the plasma profile (Fig. 7a) donepezil HCl was detected in the rat plasma after 1 h at a concentration of 28.2 ng/mL and 32.0 ng/mL for the 2.5 mg/kg and 5 mg/kg doses respectively. Concentrations progressively increased over the 24 h experiment duration, with a maximal concentration of 51.8 ± 17.6 ng/mL achieved for the higher drug loading and 35.6 ± 13.0 ng/mL for the lower loading at 24 h. The higher concentration achieved with the increased drug loading was not found to be statically different in comparison with the lower concentration ($p > 0.05$). Pharmacokinetic parameters are presented in Table 3. Css was calculated using Eq. (4), where AUC is the area under the curve and t is time.

$$\text{Css} = \frac{\text{AUC}_{0-t}}{t} \tag{4}$$

Interestingly, Tmax (Time of Maximum concentration observed) was 24 h in both rat cohorts. This may lead to a slight discrepancy of Css (steady state plasma concentration), as true steady state conditions cannot be claimed after this time period as the plasma concentrations at this time point had not plateaued. As can be seen from Fig. 7b, after 24 h the MN arrays had swollen extensively with dissolution of the donepezil HCl containing film.

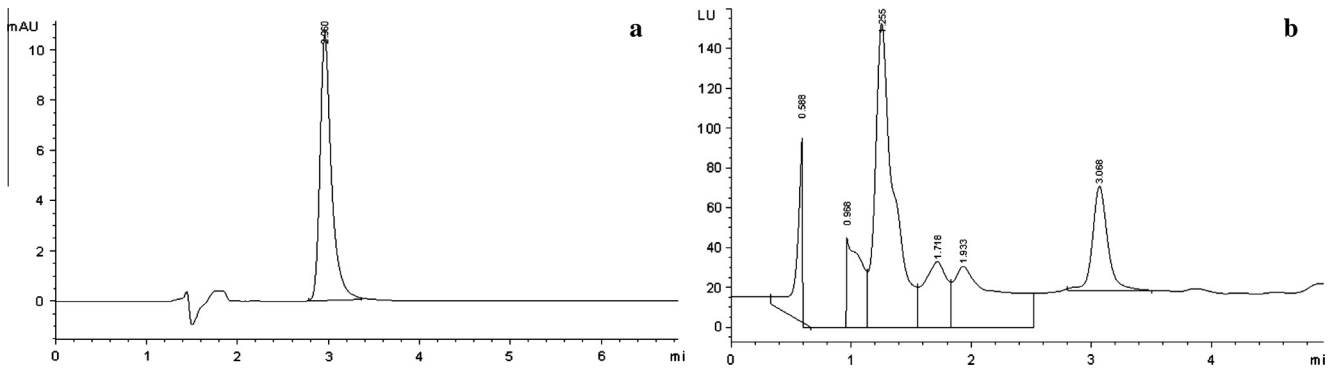

Fig. 4. Typical HPLC traces of donepezil HCl in (a) PBS and (b) rat plasma.

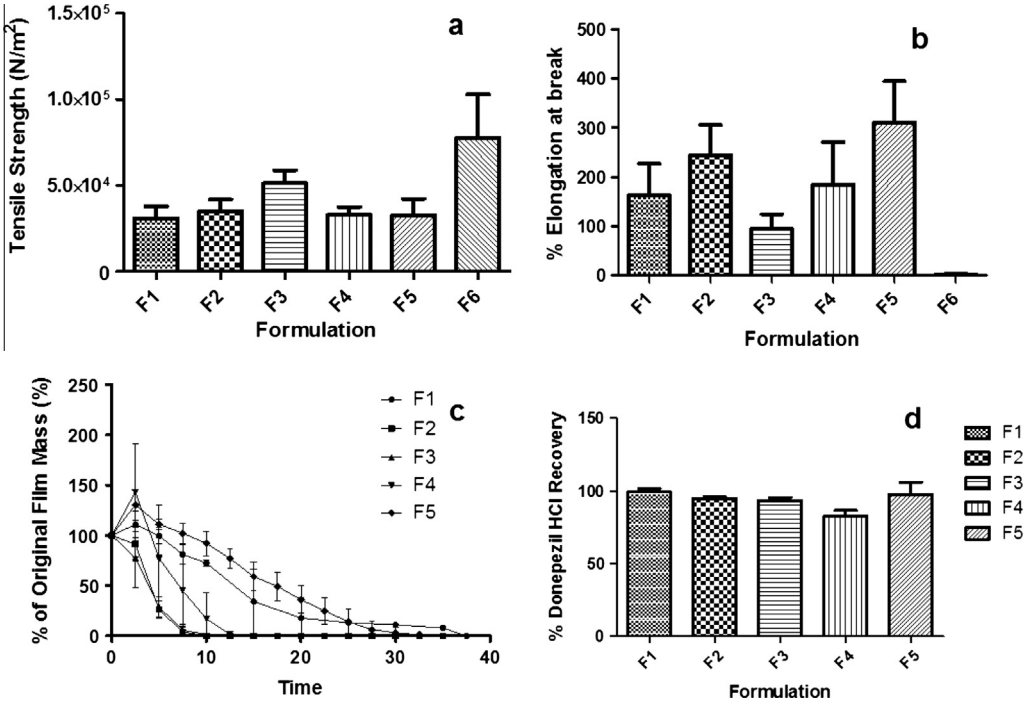

Fig. 5. Physical characterisation of donepezil HCl containing films made from formulations F1–F6: (a) tensile strength of films (means ± SD, $n = 5$), (b) percentage elongation at break of films (means ± SD, $n = 5$), (c) dissolution profile of films in PBS (7.4 pH at 25°C) (means ± SD, $n = 3$) and (d) recovery of donepezil HCl from films after dissolving in PBS and detected using RP-HPLC (means ± SD, $n = 3$).

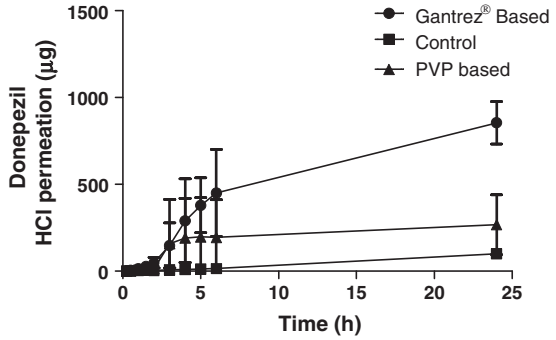

Fig. 6. *In vitro* cumulative permeation profile of donepezil HCl, across dermatomed neonatal porcine skin, from integrated patches composed of hydrogel forming MNs, and either a PVP or a PMVE/MAH-based drug loaded film (means ± SD, $n = 3$).

4. Discussion

The benefit of transdermal products for use in older populations and those affected by dementia has been well documented and confirmed by commercial success of the rivastigmine patch. Presented in this paper is the novel combination of a donepezil HCl containing film with hydrogel-forming MNs for the enhanced transdermal delivery of this Alzheimer's drug. Hydrogel-forming MNs have been shown to increase the transdermal delivery of a range of model therapeutic compounds with a diverse range of physicochemical properties [9,19,24]. This highlights the versatility of this MN design and, coupled with their self-disabling nature, hydrogel-forming MNs show considerable promise for commercial success.

When inserted into the skin, hydrogel-forming MNs swell and create a porous, aqueous network through which drug substances can diffuse through, and reach the rich dermal microcirculation below. Due to the aqueous environment created by these MNs,

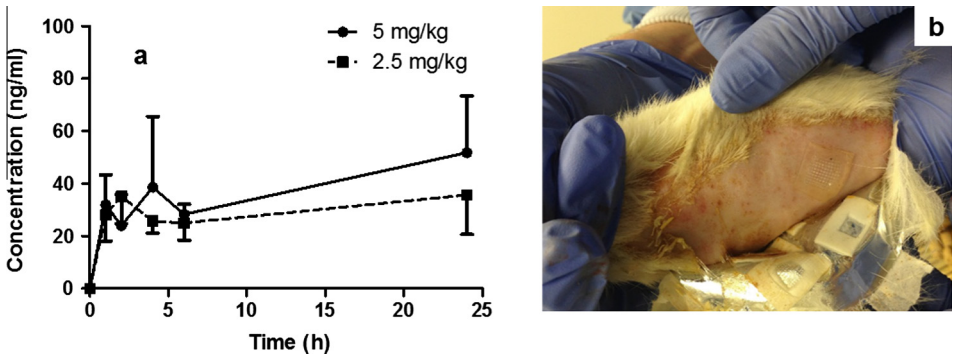

Fig. 7. (a) The *in vivo* plasma profiles of donepezil HCl (means ± SD, $n = 3$) following transdermal delivery from MN integrated patches at a dose of either 5 mg/kg or 2.5 mg/kg. (b) Digital photograph of MN array applied to the back of a rat after 24 h, with adhesive backing removed.

Table 3
Pharmacokinetic parameters of donepezil applied to rats at a dose of 3 mg/Rat or 1.5 mg/Rat (means ± SD, $n = 3$).

Parameter	5 mg/kg	2.5 mg/kg
AUC (ng h/mL)	894.5 ± 128.3	702.3 ± 142.9
Tmax (h)	24	24
Cmax (ng/mL)	51.8 ± 17.3	35.6 ± 13.0
Css (ng/mL)	37.3 ± 5.34	29.3 ± 6.0

delivery is most suited to drugs with a relatively high degree of water solubility. For this reason the HCl salt version of donepezil has been used in this study, which is in contrast to other approaches to the development of a donepezil patch, which have used the free base form [17].

The polymers selected for film preparation to be used in combination with MNs, to form an integrated patch in this study, have been previously shown to have film-forming properties [20,25]. They are biocompatible, having been used extensively in the pharmaceutical industry. These materials are water soluble and are, therefore, logical choices of polymers for this study. PVME/MAH has previously been used in combination with hydrogel-forming MNs for the delivery of the model compounds methylene blue, metronidazole and theophylline. As progression towards a commercial product continues [26], there is increasing preference for the use of the benzene free PVME/MA polymer, and as a result both were investigated [27]. With the view of modifying the release kinetics of the integrated patch, films composed of PVP with a considerably lower molecular weight than the other polymers were investigated. The mechanism of drug release from the integrated patch is diffusion; therefore, it was hypothesised that a film formed from a lower molecular weight would diffuse more rapidly than its higher molecular weight counterparts. PVP based films were therefore tested in combination with the hydrogel-forming MNs, as well as Gantrez® based films, in terms of donepezil HCl permeation.

Characterisation of the films physical properties was conducted to assess the suitability of the formulation for use in a transdermal application. The film requires a certain degree of flexibility to enable sufficient contortion to be applied to the skin, but also sufficient strength to facilitate ease of handling. Previous work has investigated the effects of various plasticisers on the physical characteristics of PMVE/MAH based films and concluded that the optimum plasticiser in films for transdermal applications is TPME [20]. Reducing the TPME concentration from 7.5% to 5% of PMVE/MAH based films significantly reduced their flexibility. It has been hypothesised that water also contributes to the plasticising effect of films containing TPME and, as the film dries upon storage the flexibility is reduced. Using the films immediately post-formulation would circumvent this, but would not make a suitable pharmaceutical product as inevitably a storage period prior to use will be necessary. To overcome this issue, heat-sealed, moisture-impermeable packaging has been used and found to be a suitable remedy [20].

In vitro permeation of donepezil HCl was assessed using the commonly employed Franz cell apparatus. A 1 cm^2 patch containing approximately 2 mg donepezil HCl delivered almost 1 mg donepezil from the integrated patch composed of hydrogel-forming MNs and F1. While it is acknowledged that porcine skin is not an exact model of human skin, it is a close replicate in terms of *stratum corneum* thickness and hair distribution [25]. As the primary barrier to transdermal delivery is the *stratum corneum*, porcine skin is therefore a suitable model membrane. Previously we have shown that the optimum skin model in terms of *in vitro* to *in vivo* was dermatomed porcine skin (thickness of 350 μm) using MNs with a height of 600 μm [25]. The integrated patch was applied to the skin with gentle pressure exerted to ensure insertion of MN tips. Following insertion, the MNs take up interstitial fluid with subsequent swelling and expansion of the hydrogel matrix, facilitating movement of molecules through the channels created in the skin. The imbibed fluid causes dissolution of the film atop the MNs with the donepezil contained within diffusing through the MNs and into the receiver compartment below. Patches containing PVP based films had significantly less permeation in comparison with Gantrez® based films ($p < 0.05$). While results of dissolution studies suggested that PVP based films dissolve more rapidly, in terms of an integrated patch, it is the rate of MN swelling that has greater influence on the dissolution of the films, as the needles must initially swell before the patch dissolves. Despite the higher flux values over the linear portions of the permeation profile for the PVP based patches, after 24 h this system did not deliver the largest amount of donepezil HCl. In fact, after 5 h, delivery from PVP-based integrated patches reached a plateau, suggesting that this system would not be suitable for a 24 h patch. Upon visual inspection of the Franz cell donor compartment post experiment, it was obvious that there was complete dissolution of the PVP-based films, yet a significantly less amount of donepezil HCl was delivered in comparison with the Gantrez®-based films ($p < 0.05$). This may possibly be attributed to the formation of hydrogen bonds between the carbonyl groups of PVP and hydroxyl groups of the PMVE/MA MNs, causing a reduction in the solubility of PVP when passing through the MNs due to reduced interaction with water molecules and potential complexation with the MN matrix itself [28].

The *in vivo* animal study has demonstrated that hydrogel-forming MNs can be used to deliver a clinically relevant drug, at therapeutically useful doses, in comparison with the many studies that investigate model compounds, offering potential for the current transdermal drug delivery market. Donepezil HCl delivered from an integrated MN patch yielded plasma concentrations in the rat model similar to the target therapeutic concentration in humans [29]. While it is acknowledged that the pharmacokinetics of a rat and a human are quite disparate, the preliminary results of this small scale study are very encouraging. When cautiously extrapolated, a human donepezil HCl dose of 5 mg/kg could be achieved with a patch size of approximately 30 cm^2. Considering an average human mass of 60 kg, it is possible to load ~160 mg donepezil HCl in 9 g formulation (9 g formulation is used to produce a film of an average thickness of 0.7 mm and area of 15 cm^2). Although it is recognised that the dose of donepezil HCl used in this experiment is much higher than the oral human dose, the numerous advantages offered by a patch formulation of donepezil make these endeavours worthwhile. Considering the delivery profile of donepezil HCl, it is notable that steady state conditions were not reached within the duration of this experiment. Saluja *et al.* have reported similar results with transdermal delivery of donepezil HCl using iontophoresis, where an average Tmax of 25.5 h was observed [18]. It is assumed that the rate of absorption is slower with transdermal delivery, and similarly there is a lag time with MN patches, as the MNs must take up interstitial fluid, the drug-loaded film dissolves, and then the drug must diffuse through the MN hydrogel matrix, prior to partition into the dermal microcirculatory system. Once the drug has diffused through the MNs, however, uptake by the dermal microcirculation is rapid [30]. With an extension of the experimental run time it would be predicted that constant plasma concentrations of donepezil would be maintained, as the MNs had reached a state of maximum swelling at 24 h, and the donepezil would move through the swollen MNs and be taken up by the rich dermal microcirculation until depletion of the reservoir patch and diffusion through the array. The duration of the *in vivo* study was kept to a minimum due to a restriction in blood sampling volumes within a given time period, as well as considering the aim of the study, which was to establish

preliminary data to demonstrate the enhanced transdermal delivery of donepezil HCl. We have provided 'proof of concept' evidence that donepezil HCl can be delivered *in vivo* using hydrogel-forming MNs.

5. Conclusion

This study has demonstrated the *in vitro* and *in vivo* delivery of donepezil HCl *via* hydrogel forming MNs. This is the first report of the effective transdermal delivery of donepezil, using a convenient MN formulation. As the field of MN technology progresses it is important that due consideration is given to the types of drugs that will be delivered using this platform. Future work will involve *in vivo* sampling beyond 24 h as well as more extensive pharmacokinetic analysis to enable progression towards a clinical application. By further modification of the MN and/or reservoir patch formulation, this integrated patch could be optimised to offer a range of doses over varying time periods. The benefit of transdermal products in the treatment of Alzheimer's disease is well documented and this study offers substantial promise in the attainment of a donepezil patch.

Acknowledgements

This study was supported by the Engineering & Physical Sciences Research Council, Grant number 1347368.

References

[1] A. Arora, M.R. Prausnitz, S. Mitragotri, Micro-scale devices for transdermal drug delivery, Int. J. Pharm. 364 (2008) 227–236, http://dx.doi.org/10.1016/j.ijpharm.2008.08.032.
[2] J.R. Walter, S. Xu, Therapeutic transdermal drug innovation from 2000 to 2014: current status and outlook, Drug Discov. Today (2015), http://dx.doi.org/10.1016/j.drudis.2015.06.007.
[3] S. Henry, D. McAllister, M. Allen, M. Prausnitz, Microfabricated microneedles: a novel approach to transdermal drug delivery, J. Pharm. Sci. 88 (1999) 948, http://dx.doi.org/10.1021/js990783q.
[4] T.-M. Tuan-Mahmood, M.T.C. McCrudden, B.M. Torrisi, E. McAlister, M.J. Garland, T.R.R. Singh, et al., Microneedles for intradermal and transdermal drug delivery, Eur. J. Pharm. Sci. 50 (2013) 623–637, http://dx.doi.org/10.1016/j.ejps.2013.05.005.
[5] K. Cheung, D.B. Das, Microneedles for drug delivery: trends and progress, Drug Deliv. 25 (2014) 1–17.
[6] S. Hirobe, H. Azukizawa, T. Hanafusa, K. Matsuo, Y.-S. Quan, F. Kamiyama, et al., Clinical study and stability assessment of a novel transcutaneous influenza vaccination using a dissolving microneedle patch, Biomaterials 57 (2015) 50–58, http://dx.doi.org/10.1016/j.biomaterials.2015.04.007.
[7] H.L. Quinn, M.-C. Kearney, A.J. Courtenay, M.T. McCrudden, R.F. Donnelly, The role of microneedles for drug and vaccine delivery, Expert Opin. Drug Deliv. 11 (2014) 1769–1780.
[8] S. Indermun, R. Luttge, Y.E. Choonara, P. Kumar, L.C. du Toit, G. Modi, et al., Current advances in the fabrication of microneedles for transdermal delivery, J. Control. Release 185 (2014) 130–138, http://dx.doi.org/10.1016/j.jconrel.2014.04.052.
[9] R.F. Donnelly, T.R.R. Singh, M.J. Garland, K. Migalska, R. Majithiya, C.M. McCrudden, et al., Hydrogel-forming microneedle arrays for enhanced transdermal drug delivery, Adv. Funct. Mater. 22 (2012) 4879–4890, http://dx.doi.org/10.1002/adfm.201200864.
[10] S. Wiedersberg, R.H. Guy, Transdermal drug delivery: 30+ years of war and still fighting!, J Control. Release 190 (2014) 150–156, http://dx.doi.org/10.1016/j.jconrel.2014.05.022.
[11] R.H. Affoo, N. Foley, J. Rosenbek, J.K. Shoemaker, R.E. Martin, Swallowing dysfunction and autonomic nervous system dysfunction in Alzheimer's disease: a scoping review of the evidence, J. Am. Geriatr. Soc. 61 (2013) 2203–2213, http://dx.doi.org/10.1111/jgs.12553.
[12] C.M. Roe, M.J. Anderson, B. Spivack, How many patients complete an adequate trial of donepezil?, Alzheimer Dis Assoc. Disord. 16 (2002) 49–51.
[13] J.F. Burris, V. Papademetriou, J.D. Wallin, M.E. Cook, D.J. Weidler, Therapeutic adherence in the elderly: transdermal clonidine compared to oral verapamil for hypertension, Am. J. Med. 91 (1991) S22–S28, http://dx.doi.org/10.1016/0002-9343(91)90059-7.
[14] V. Vagenas, G.S. Vlachos, N. Vlachou, D. Liakopoulos, M.E. Kalaitzakis, M. Vikelis, A prospective non-interventional study for evaluation of quality of life in patients with Alzheimer's disease treated with rivastigmine transdermal patch, SAGE Open Med. 3 (2015), http://dx.doi.org/10.1177/2050312115587795. 2050312115587795.
[15] Z. Xia, X. Jiang, X. Mu, H. Chen, Improvement of microemulsion electrokinetic chromatography for measuring octanol–water partition coefficients, Electrophoresis 29 (2008) 835–842, http://dx.doi.org/10.1002/elps.200700104.
[16] J. Choi, M.-K. Choi, S. Chong, S.-J. Chung, C.-K. Shim, D.-D. Kim, Effect of fatty acids on the transdermal delivery of donepezil: in vitro and in vivo evaluation, Int. J. Pharm. 422 (2012) 83–90, http://dx.doi.org/10.1016/j.ijpharm.2011.10.031.
[17] K.H. Kim, H.S. Gwak, Effects of vehicles on the percutaneous absorption of donepezil hydrochloride across the excised hairless mouse skin, Drug Dev. Ind. Pharm. 37 (2011) 1125–1130, http://dx.doi.org/10.3109/03639045.2011.561352.
[18] S. Saluja, P.C. Kasha, J. Paturi, C. Anderson, R. Morris, A.K. Banga, A novel electronic skin patch for delivery and pharmacokinetic evaluation of donepezil following transdermal iontophoresis, Int. J. Pharm. 453 (2013) 395–399, http://dx.doi.org/10.1016/j.ijpharm.2013.05.029.
[19] R.F. Donnelly, M.T.C. McCrudden, A. Zaid Alkilani, E. Larrañeta, E. McAlister, A.J. Courtenay, et al., Hydrogel-forming microneedles prepared from "super swelling" polymers combined with lyophilised wafers for transdermal drug delivery, PLoS One 9 (2014) e111547, http://dx.doi.org/10.1371/journal.pone.0111547.
[20] P.A. McCarron, A.D. Woolfson, R.F. Donnelly, G.P. Andrews, A. Zawislak, J.H. Price, Influence of plasticizer type and storage conditions on properties of poly (methyl vinyl ether-co-maleic anhydride) bioadhesive films, J. Appl. Polym. Sci. 91 (2004) 1576–1589.
[21] ICH, International conference on harmonisation of technical requirements for registration of pharmaceuticals for human use, ICH Harmon. Tripart. Guidel. Anal. Proced. Text Methodol. (2005).
[22] M.T.C. McCrudden, A.Z. Alkilani, C.M. McCrudden, E. McAlister, H.O. McCarthy, A.D. Woolfson, et al., Design and physicochemical characterisation of novel dissolving polymeric microneedle arrays for transdermal delivery of high dose, low molecular weight drugs, J. Control. Release 180C (2014) 71–80, http://dx.doi.org/10.1016/j.jconrel.2014.02.007.
[23] M.J. Garland, K. Migalska, T.M. Tuan-Mahmood, T. Raghu Raj Singh, R. Majithija, E. Caffarel-Salvador, et al., Influence of skin model on in vitro performance of drug-loaded soluble microneedle arrays, Int. J. Pharm. 434 (2012) 80–89, http://dx.doi.org/10.1016/j.ijpharm.2012.05.069.
[24] M.J. Garland, E. Caffarel-Salvador, K. Migalska, a.D. Woolfson, R.F. Donnelly, Dissolving polymeric microneedle arrays for electrically assisted transdermal drug delivery, J. Control. Release 159 (2012) 52–59, http://dx.doi.org/10.1016/j.jconrel.2012.01.003.
[25] S. Gaisford, A. Verma, M. Saunders, P.G. Royall, Monitoring crystallisation of drugs from fast-dissolving oral films with isothermal calorimetry, Int. J. Pharm. 380 (2009) 105–111, http://dx.doi.org/10.1016/j.ijpharm.2009.07.006.
[26] R.E.M. Lutton, E. Larrañeta, M.-C. Kearney, P. Boyd, A.D. Woolfson, R.F. Donnelly, A novel scalable manufacturing process for the production of hydrogel-forming microneedle arrays, Int. J. Pharm. 494 (2015) 417–429, http://dx.doi.org/10.1016/j.ijpharm.2015.08.049.
[27] ICH Expert Working Group, Impurities: Guideline for Residual Solvents Q3C (R5), 2011.
[28] J.S. Hao, L.W. Chan, Z.X. Shen, P.W.S. Heng, Complexation between PVP and Gantrez polymer and its effect on release and bioadhesive properties of the composite PVP/Gantrez films, Pharm. Dev. Technol. 9 (2004) 379–386, http://dx.doi.org/10.1081/PDT-200033004.
[29] S.L. Rogers, R.S. Doody, R.C. Mohs, L.T. Friedhoff, Donepezil improves cognition and global function in Alzheimer disease, Arch. Intern. Med. 158 (1998) 1021–1031.
[30] H.A.E. Benson, A.C. Watkinson, Topical and Transdermal Drug Delivery: Principles and Practice, Wiley, Oxford, 2012, ISBN 978-0-470-45029-1.